THE JOURNAL OF PHYSICAL CHEMISTRY A LETTERS

2009, *113,* 629–632
Published on Web 01/08/2009

Onset of Double Helical Structure in Small-Sized Homoleptic Gold Thiolate Clusters

Nan Shao, Yong Pei, Yi Gao, and Xiao Cheng Zeng*

Department of Chemistry and Nebraska Center for Materials and Nanoscience, University of Nebraska, Lincoln, Nebraska 68588

Received: November 28, 2008

Low-lying isomers of homoleptic gold thiolate clusters $(AuSR)_N$ ($N = 6-12$) are studied by using a global-minimum search method. Besides previously known zigzag crown structures for $(AuSR)_N$ ($N = 6-12$) and catenane structures for $(AuSR)_N$ ($N = 10, 12$), onset of a new structural family of double helical structures in small-sized gold thiolate clusters and the separate-ring structures in larger clusters is revealed. At $N = 6-9$, the double helical structures are predicted to be the global minima. The onset of double helical structures suggests a new folding way for flexible gold thiolate clusters. The simulated UV−vis spectra and XRD patterns for all low-lying clusters are ready to compare with future experiments.

Ligand-protected gold nanoparticles (AuNP) have attracted considerable interest because of their promising applications in nanocatalysis, medicine, and optical devices.[1,2] Recently, two major breakthroughs were made in total structure determination of thiolate-protected gold clusters, namely, $Au_{102}(p\text{-MBA})_{44}$ and $Au_{25}(SR)_{18}^-$.[3,4] In both clusters, the gold core exhibits unusually high symmetry, contrasting to the core of bare gold clusters at the same size. More significantly, the notion of "staple motif" is firmly established based on $Au_{102}(p\text{-MBA})_{44}$ and $Au_{25}(SR)_{18}^-$.[3,4] This notion has been applied to predict the structure of $Au_{38}(SR)_{24}$.[5] Despite major progress in resolving the structure of thiolated-protected gold clusters, structural evolution of gold thiolate clusters in general is still largely unknown because of limited experimental data on structures of gold thiolate clusters in the small-to-medium size range.[2−4]

For thiolate-protected gold clusters, the gold-to-thiolate ratio is usually greater than 1:1. In this case, either the simple "staple motifs" -*RS*-Au-*RS*- and/or the extended motifs -*RS*-Au-*RS*-Au-*RS*- can entirely cover an inner Au core.[3−7] Also, the electronic shell model has been used to explain the exceptional stability of certain (magic) thiolate-protected gold clusters.[3−7] However, for the homoleptic type of gold thiolate clusters $(AuSR)_N$ with an exactly 1:1 gold-to-thiolate ratio, previous studies were limited only to small clusters such as $[AuSC(SiMe_3)_3]_4$.[8] The small-sized clusters were proposed to be intermediates of growing clusters, based on high yield of glutathione gold clusters $[AuSG]_N$ ($N = 10-12$) detected in the mass spectrometry experiment.[9] In homoleptic-type $[AuSR]_N$, the Au and S atoms have two- and three-coordination, respectively, resulting in enormous conformational flexibility. Indeed, Elder et al. reported both open-chain and closed-chain structures of myochrisin, a gold thiolate complex with six gold atoms.[10a] LeBlanc and Lock achieved crystallization of $(AuSC_{15}H_{23})_6C_4H_{10}O$, which has a chairlike structure.[10b] Other intriguing homoleptic structures previously found were gold thiolate catenanes such as $[Au(SC_6H_4\text{-}p\text{-}CMe_3)]_{10}$ and $[Au(SC_6H_4\text{-}o\text{-}CMe_3)]_{12}$.[11] The $[Au(SC_6H_4\text{-}p\text{-}CMe_3)]_{10}$ has two interpenetrated pentagons, each having five S atoms and five Au atoms, with the sixth Au atom located at each pentagon center. A similar catenane structure was seen in the $[Au(SC_6H_4\text{-}o\text{-}CMe_3)]_{12}$ cluster. An ab initio theoretical study of $(AuSR)_N$ ($N = 2-12$) clusters by Grönbeck et al.[12] predicted a transition from a planar cyclic to zigzag crown structure with increasing cluster size.

In this letter, we report a systematic ab initio study of low-lying structures of homoleptic $(AuSR)_N$, $N = 6-12$. Major attention is placed on the search for structures of the lowest-energy clusters of $(AuSR)_N$, $N = 6-12$. To this end, we devised a two-step computational approach. First, an unbiased global search is undertaken to search for the lowest-energy clusters $(AuSH)_N$, using the basin-hopping (BH)[13] method combined with density functional theory (DFT) geometric optimization. Specifically, the gradient-corrected Perdew−Burke−Ernzerh (PBE) exchange-correlation functional[14] and the double-numerical polarized (DNP) basis set with effective core potential (ECP), implemented in DMOL3 software,[15] were chosen for the global minimum search and geometric optimization. Second, the H atoms in the low-lying clusters obtained in step one were replaced by methyl groups, followed by reranking the low-lying $(AuSR)_N$ clusters using the DFT/PBE method with two different basis sets, (1) the DNP basis set, implemented in DMOL3 software and (2) the Lanl2dz ECP for Au and the all-electron 6-311G(d) basis set for S, C, and H, implemented in GAUSSIAN03 package.[16] Harmonic vibrational frequencies (Table S1, Supporting Information) were then computed at the PBEPBE/Lanl2dz (Au) and 6-311G(d) (S, C, and H) level of theory to ensure that the optimized structures were true local minima without imaginary frequencies. As shown in Table S1 (Supporting Information), the computed relative energies are sensitive to the basis sets selected. Consequently, all low-lying isomers with relative energies within a few kcal/mol from the lowest-energy isomer can be considered as candidates for the global minimum. To better determine true global minima, we employed the second-order Moller−Plesset perturbation (MP2)[17] method to compute the single-point energies (see Figure 1) for all low-

* To whom correspondence should be addressed. E-mail: xczeng@phase2.unl.edu.

10.1021/jp810447k CCC: $40.75

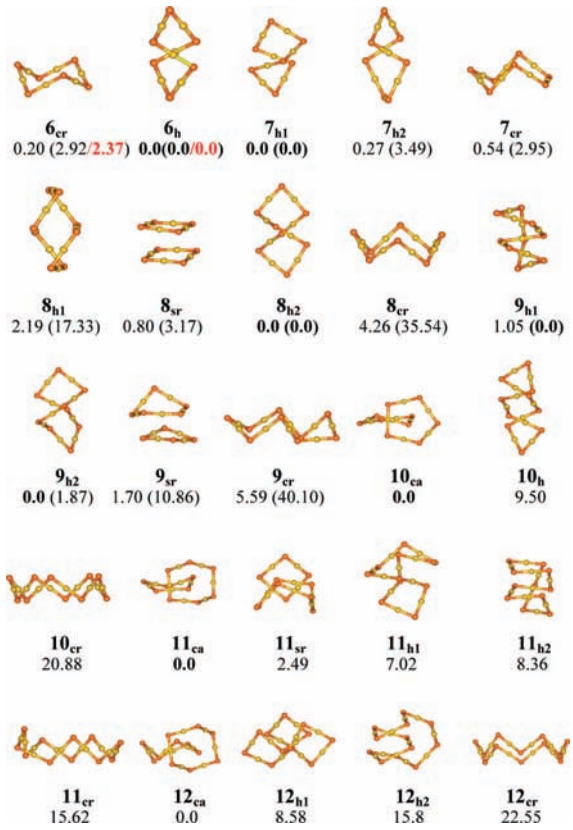

Figure 1. Optimized structures of low-lying isomers of $(AuSCH_3)_N$ ($N = 6-12$). The methyl groups are not displayed for clarity. The subscripts are h: helix, cr: crown, ca: catenane, sr: seperate ring. The relative energies (kcal/mol) are computed based on optimization at PBEPBE/LANL2DZ (Au) and the 6-311G(d) (S,C,H) level of theory.[16] Relative MP2 single-point energies calculated with the SDD(f) (Au) and 6-311G(d) (S, C, and H) basis sets are given in parentheses. MP4(SDQ) relative energies with the SDD(f) (Au) and 6-311G(d) (S, C, and H) basis sets are highlighted in red. Color code of atoms: orange (S), gold (Au).

lying clusters in the size range of $N = 6-9$, based on their geometry optimized at the PBEPBE/Lanl2dz(Au)/6-311G(d-)(S,C,H) level of theory. Additionally, for $N = 6$, the fourth-order Moller−Plesset perturbation with the single, double, and quadruple substitution [MP4(SDQ)] method was used to confirm that the MP2 relative energies were qualitatively correct. For both MP2 and MP4 calculations, the Stuttgart/Dresden (SDD)[18] basis set augmented by one set of f polarization functions (exponent = 1.056) was used for Au, and 6-311G(d) basis set was used for S, C, and H.

The global minimum search reveals a new structural family of double helical gold thiolate clusters which are energetically competitive compared to the known zigzag crown structures. The onset of double helical structure in small-sized gold thiolate clusters suggests a new folding manner for flexible gold thiolate clusters, as well as a new path of one-dimensional (1D) growth in the structural evolution of gold thiolate clusters. Note that the double helical gold thiolate structure has been previously found but only in the solid state, that is, polymeric four-fold helical gold thiomalate (myochrysine).[19a] Possible existence of small double helical gold thiolate fragments in solution was also proposed. The double helical structures were also found in the silver thiolate, for example, in the $[AgSC(CH_3)(C_2H_5)_2]_N$ crystal, although it is eight-fold in structure.[19b]

Figure 1 displays all low-lying isomers of $(AuSCH_3)_N$, $N = 6-12$, which exhibit four types of structures, namely, double

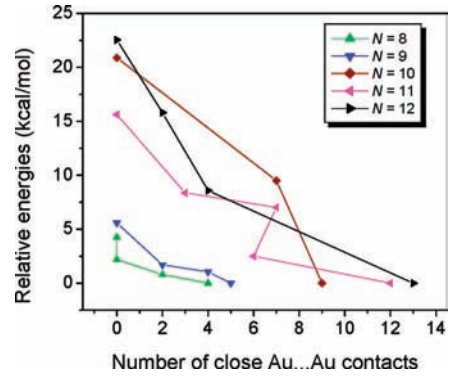

Figure 2. ΔE versus the number of close Au−Au contacts in low-lying isomers of $(AuSCH_3)_N$, ($N = 8-12$). The relative energies (kcal/mol) are computed based on optimization at PBEPBE/LANL2DZ (Au) and the 6-311G(d) (S,C,H) level of theory.[16] Close Au···Au contacts are defined as those Au−Au pairs whose intrapair distance is in the range of 3.9−4 Å.

helical, crown, catenane, and separate rings. Interestingly, for $N = 6-9$, the predicted global minima are all double helical clusters which have lower energy than the crown isomers (at both DFT and MP2 levels; for $N = 6$, at the MP4 level as well). For larger $(AuSCH_3)_N$, $N = 10-12$, the catenane structure becomes the most stable one, followed by the double helical and crown structures.[12] The fourth type of structure, the separate rings, may be viewed as an intermediate between closed-chain (crown and double helical) and catenane isomers. It is expected that beyond certain size (N), the closed-chain clusters will eventually break and turn into separate rings. This is because the six-membered crown structure is highly stable, followed by the five- and seven-membered crown structures. Hence, the breaking size is likely at $N \sim 10-14$. When separate rings can reduce the total energy at close distance, the two rings tend to fuse together to form a catenane.

Relative energies at 0 K are given in Figure 1. To evaluate the temperature effect on the stability of clusters, Gibbs energy corrections (based on harmonic approximation) from 0 to 800 K are computed. The Gibbs free energies versus temperature curves for all candidate isomers are shown in the Supporting Information. It is found that at room temperature, the ranking of isomers based on total Gibbs energies is generally the same as that based electronic energies. However, above 650 K, $(AuSCH_3)_{10}$-double helix may become more stable than $(AuSCH_3)_{10}$-catenane. The HOMO−LUMO (H−L) gap for each cluster shown in Figure 1 is given in Supporting Information Table S1, and the H−L gap decreases with increasing cluster sizes. The crown structures appear to have larger H−L gaps than other isomeric structures.

The double helical, crown, catanene, and separate-ring structures shown in Figure 1 can be viewed as various combinations of a series of simple "staple motif" -*RS*-Au-*RS*-. Here, the S atom in the simple staple motif has sp^3 hybridization. A lone pair of S atoms is involved in the Au−S bonding. We find that for all double helical structures shown in Figure 1, the Au−S−Au angle is merely ~90°, much less than 109.5° in the general case of sp^3 hybridization, an indicator of strong Au···Au interaction. Indeed, the strong Au···Au interaction was previously suggested to be responsible for the stability of closed-chain gold thiolate $[Au(SC_6H_4\text{-}p\text{-}CMe_3)]_{10}$.[11] Moreover, the energy ranking of low-lying isomers appears to be correlated with the number of close Au···Au contacts (Figure 2), which can be defined as those Au−Au pairs with an intrapair distance within 3.9−4 Å (the cutoff distances depend somewhat on the

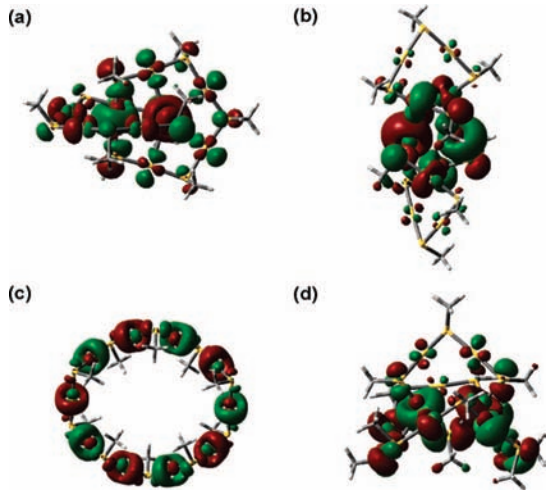

Figure 3. HOMO of the low-lying isomers; (a) $(AuSCH_3)_{10}$-catenane, (b) $(AuSCH_3)_{10}$-helix, (c) $(AuSCH_3)_{10}$-crown, and (d) $(AuSCH_3)_{11}$-seperate ring. The structures are optimized at PBEPBE/LANL2DZ (Au) and the 6-311G(d) (S,C,H) level of theory.

functional and basis sets used for geometry optimization). Here, the close Au···Au contact excludes all next-nearest-neighbor Au−Au pairs, whose number (N) is identical for every isomer. As such, except for $(AuSCH_3)_6$ and $(AuSCH_3)_7$, which have no close Au···Au contact, all $(AuSCH_3)_N$, $N = 8-12$, show inverse proportion of the relative electronic energy ΔE to the number of close Au···Au contacts. In other words, the larger number of close Au···Au contacts, the lower ΔE. For $(AuSCH_3)_N$, $N = 8-9$, the lowest-energy double helical structures have the largest number of close Au···Au contacts. For $(AuSCH_3)_N$, $N = 10-12$, the catanene structures give rise to largest number of close Au···Au contacts, resulting in lower energies. The only exception is $(AuSCH_3)_{11}$-h1 (Figure 2), which is 4.53 kcal/mol higher in energy than $(AuSCH_3)_{11}$-sr but with one more close Au···Au contact.

Catenane $(AuSR)_{11}$ (R = H or CH_3) was considered to be the lowest-energy isomer as in the case of catenane $(AuSR)_{10}$ and $(AuSR)_{12}$. However, it turns out that its stability over other isomers is not as high as $(AuSR)_{10}$ and $(AuSR)_{12}$. Hence, the catenane $(AuSR)_{11}$ may be difficult to isolate in experiment. Catenane $(AuSH)_9$ is found to be unstable upon structural optimization.

Representative Kohn−Sham HOMO orbitals for $(AuSCH_3)_{10}$-catenane, $(AuSCH_3)_{10}$-helix, $(AuSCH_3)_{10}$-crown, and $(AuSCH_3)_{11}$-seperate ring are plotted in Figure 3. For the crown structure (Figure 3c), the Au(d)−S(p) hybridization gives rise to covalent bonding feature of the Au−S bond, similar to the crown structure of $(AuSCH_3)_4$.[12] The HOMO of catenane $(AuSCH_3)_{10}$ exhibits notable s and d orbital features of two Au atoms in each center, as well as p orbitals of S atoms that connect to the two central Au atoms. For $(AuSCH_3)_{10}$-helix, the HOMO is mainly contributed to by the s and d orbitals of three Au atoms in the middle screwy part and the p orbitals of central S atoms (50.45%). It appears that the hybridization among these orbitals at the central region enhances the stability of the double helical structure. The HOMO of the separate-ring structure (Figure 3 d) is mainly contributed to by two central Au atoms. This isomer has seven close contacts but little contact between two central Au atoms. The central Au atoms in catenane $(AuSCH_3)_{10}$ have a total of nine close contacts with other Au atoms, including one between themselves.

The double helical structure has a relatively smaller mean Au−Au distance (D_{Au-Au}) compared to that of other isomers

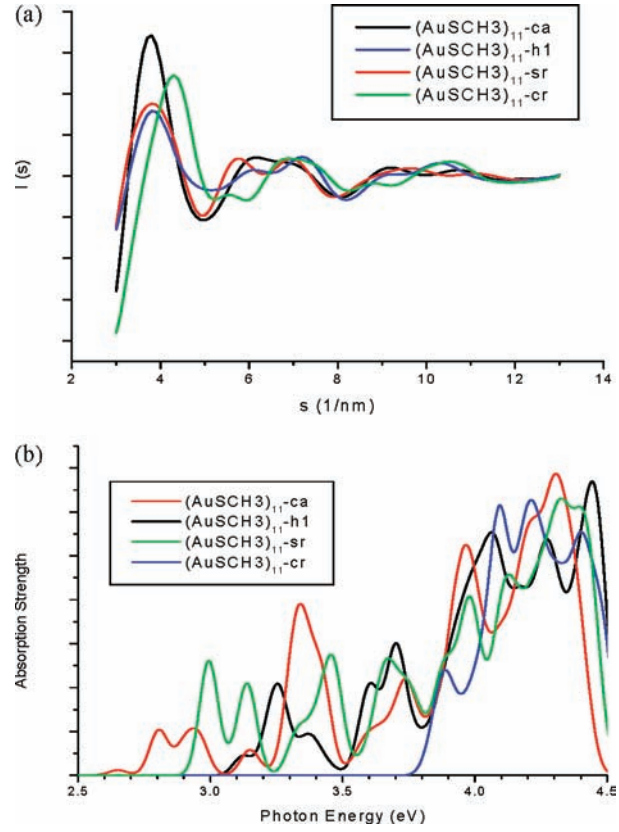

Figure 4. Simulated (a) XRD patterns and (b) UV−vis optical spectra of various isomers; $(AuSCH_3)_{11}$-catenane, $(AuSCH_3)_{11}$-helix, $(AuSCH_3)_{11}$-crown, and $(AuSCH_3)_{11}$-seperate ring are presented in red, black, green, and blue, respectively.

(see Supporting Information Table S2). The D_{Au-Au} distance is an important indicator to characterize the stability of gold thiolate. The isomer with the lowest energy has the least D_{Au-Au} when $N = 6 - 8$, 10, and 11. Nevertheless, it is not always true that the shorter D_{Au-Au} the higher the stability of isomer. For example, catenane $(AuSCH_3)_9$ is unstable even though it has the shortest 3.0 Å D_{Au-Au}. $(AuSCH_3)_{11}$-seperate ring has a comparable D_{Au-Au} as the catenane isomer, while $(AuSCH_3)_{12}$-helix1 has a shorter D_{Au-Au} (by 0.03 Å) than that of $(AuSCH_3)_{12}$-catenane.

The simulated XRD patterns[4a,20] of selected isomers are shown in Figure 4a. It can be seen that $(AuSCH_3)_{11}$-catenane has the highest first peak. $(AuSCH_3)_{11}$-helix and $(AuSCH_3)_{11}$-seperate ring have similar first-peak positions at 3.8 nm^{-1}, while $(AuSCH_3)_{11}$-crown has a longer diffraction vector length at 4.3 nm^{-1} for the first peak. These XRD patterns are readily compared with future measurements. The UV−vis optical absorption spectrum for each isomer of $(AuSCH_3)_{11}$ is also computed[21] and plotted in Figure 4b. The optical gaps seem consistent with the H−L gaps, and the differences between them are less than 0.08 eV. The crown $(AuSCH_3)_{11}$ has the largest optical gap (~3.89 eV). The optical spectra may be used to compare experiments for assigning isomer structures. The simulated XRD patterns and UV−vis spectra for other low-lying isomers are given in the Supporting Information Figures S2a and S2(b).

In conclusion, we have performed a global minimum search for the low-lying structures of gold thiolate clusters with gold atoms ranging from 6 to 12. The energy ranking for all low-lying isomers was obtained (at both DFT and MP2 level). A new structural family of double helical clusters was revealed

for the first time in homoleptic gold thiolate clusters. At $N = 6-9$, the double helical structure is the global minimum. The HOMO of double helical clusters is mainly contributed to by the s and d orbitals of Au atoms in the middle screwy part and the p orbitals of central S atoms. It appears that the hybridization among these orbitals at the central region results in more close Au···Au contacts and enhances the stability of the double helical structure. The onset of double helical structures in small-sized clusters suggests a new folding way for flexible gold thiolate clusters.

Acknowledgment. This work was supported by grants from NSF (CHEM, CMMI and DMR/MRSEC), ARO, the Nebraska Research Initiative, and by the Research Computing Facility at University of Nebraska—Lincoln and the Holland Supercomputing Center in University of Nebraska—Omaha.

Supporting Information Available: Formula for XRD calculation, relative energies, frequencies, HOMO−LUMO gaps, computed optical spectra, XRD spectra, and coordinates of low-lying isomers. This material is available free of charge via the Internet at http://pubs.acs.org.

References and Notes

(1) (a) Brust, M.; Walker, M.; Bethell, D.; Schiffrin, D. J.; Whyman, R. *J. Chem. Soc., Chem. Commum.* **1994**, 801. (b) Whetten, R. L.; Khoury, J. T.; Alvarez, M. M.; Murthy, S.; Vezmar, I.; Wang, Z. L.; Stephens, P. W.; Cleverland, C. L.; Luedtke, W. D.; Landman, U. *Adv. Mater.* **1996**, *8*, 428.

(2) (a) Templeton, A. C.; Wuelfing, W. P.; Murray, R. W. *Acc. Chem. Res.* **2000**, *33*, 27. (b) Woehrle, G. H.; Warner, M. G.; Hutchison, J. *J. Phys. Chem. B* **2002**, *106*, 9979. (c) Daniel, M.-C.; Astruc, D. *Chem. Rev.* **2004**, *104*, 293.

(3) Jadzinsky, P. D.; Calero, G.; Ackerson, C. J.; Bushnell, D. A.; Kornberg, R. D. *Science* **2007**, *318*, 430.

(4) (a) Heaven, M. W.; Dass, A.; White, P. S.; Holt, K. M.; Murray, R. W. *J. Am. Chem. Soc.* **2008**, *130*, 3754. (b) Akola, J.; Walter, M.; Whetten, R. L.; Häkkinen, H.; Grönbeck, H. *J. Am. Chem. Soc.* **2008**, *130*, 3756. (c) Zhu, M.; Aikens, C. M.; Hollander, F. J.; Schatz, G. C.; Jin, R. *J. Am. Chem. Soc.* **2008**, *130*, 5883.

(5) (a) Pei, Y.; Gao, Y.; Zeng, X. C. *J. Am. Chem. Soc.* **2008**, *130*, 7830. (b) Jiang, D.-E.; Tiago, M. L.; Luo, W.; Dai, S. *J. Am. Chem. Soc.* **2008**, *130*, 2777.

(6) Gao, Y.; Shao, N.; Zeng, X. C. *ACS Nano* **2008**, *2*, 1497.

(7) Walter, M.; Akola, J.; Lopes-Acevedo, O.; Jadzinsky, P. D.; Calero, G.; Ackerson, C. J.; Whetten, R. L.; Grönbeck, H.; Häkkinen, H. *Proc. Natl. Acad. Sci. U.S.A.* **2008**, *105*, 9157.

(8) Bonasia, P. J.; Gindelberger, D. E.; Arnold, J. *Inorg. Chem.* **1993**, *32*, 5126.

(9) Negishi, Y.; Nobusada, K.; Tsukuda, T. *J. Am. Chem. Soc.* **2005**, *127*, 5261.

(10) (a) Elder, R. C.; Ludwig, K.; Cooper, J. N.; Eidsness, M. K. *J. Am. Chem. Soc.* **1985**, *107*, 5024. (b) LeBlanc, D. J.; Lock, C. J. L. *Acta Crystallogr.* **1997**, *C53*, 1765.

(11) Wiseman, M. R.; Marsh, P. A.; Bishop, P. T.; Brisdon, B. J.; Mahon, M. F. *J. Am. Chem. Soc.* **2000**, *122*, 12598.

(12) Grönbeck, H.; Whetten, R. L.; Häkkinen, H. *J. Am. Chem. Soc.* **2006**, *128*, 10268.

(13) Wales, D. J.; Scheraga, H. A. *Science* **1999**, *285*, 1368.

(14) Perdew, J. P.; Burke, K.; Ernzerhof, M. *Phys. Rev. Lett.* **1996**, *77*, 3865.

(15) (a) Delley, B. *J. Chem. Phys.* **1990**, *92*, 508. (b) Delley, B. *J. Chem. Phys.* **2000**, *113*, 7756.

(16) Frisch, M. J.; Trucks, G. W.; Schlegel, H. B.; Scuseria, G. E.; Robb, M. A.; Cheeseman, J. R.; Montgomery, J. A., Jr.; Vreven, T.; Kudin, K. N.; Burant, J. C.; Millam, J. M.; Iyengar, S. S.; Tomasi, J.; Barone, V.; Mennucci, B.; Cossi, M.; Scalmani, G.; Rega, N.; Petersson, G. A.; Nakatsuji, H.; Hada, M.; Ehara, M.; Toyota, K.; Fukuda, R.; Hasegawa, J.; Ishida, M.; Nakajima, T.; Honda, Y.; Kitao, O.; Nakai, H.; Klene, M.; Li, X.; Knox, J. E.; Hratchian, H. P.; Cross, J. B.; Bakken, V.; Adamo, C.; Jaramillo, J.; Gomperts, R.; Stratmann, R. E.; Yazyev, O.; Austin, A. J.; Cammi, R.; Pomelli, C.; Ochterski, J. W.; Ayala, P. Y.; Morokuma, K.; Voth, G. A.; Salvador, P.; Dannenberg, J. J.; Zakrzewski, V. G.; Dapprich, S.; Daniels, A. D.; Strain, M. C.; Farkas, O.; Malick, D. K.; Rabuck, A. D.; Raghavachari, K.; Foresman, J. B.; Ortiz, J. V.; Cui, Q.; Baboul, A. G.; Clifford, S.; Cioslowski, J.; Stefanov, B. B.; Liu, G.; Liashenko, A.; Piskorz, P.; Komaromi, I.; Martin, R. L.; Fox, D. J.; Keith, T.; Al-Laham, M. A.; Peng, C. Y.; Nanayakkara, A.; Challacombe, M.; Gill, P. M. W.; Johnson, B.; Chen, W.; Wong, M. W.; Gonzalez, C.; Pople, J. A. *Gaussian 03*; Gaussian, Inc.: Wallingford, CT, 2004; *GaussView 3.0*; Gaussian, Inc.: Pittsburgh, PA, 2002.

(17) (a) Moller, C.; Plesset, M. S. *Phys. Rev.* **1934**, *46*, 618. (b) Head-Gordon, M.; Pople, J. A.; Frisch, M. J. *Chem. Phys. Lett.* **1988**, *153*, 503.

(18) Dolg, M.; Wedig, U.; Stoll, H.; Preuss, H. *J. Chem. Phys.* **1987**, *86*, 866.

(19) (a) Bau, R. *J. Am. Chem. Soc.* **1998**, *120*, 9380. (b) Dance, I. G.; Fitzpatrick, L. J.; Rae, A. D.; Scudder, M. L. *Inorg. Chem.* **1983**, *22*, 3785.

(20) Cleveland, C. L.; Landman, U.; Shafigullin, M. N.; Stephens, P. W.; Whetten, R. L. *Z. Phys. D* **1997**, *40*, 503.

(21) ADF 2007.01; SCM Theoretical Chemistry, Vrije Universiteit: The Netherlands, http://www.scm.com.

JP810447K